








Manganese-Enhanced Magnetic Resonance Imaging in Takotsubo Syndrome

Trisha Singh¹ , BM; Shruti Joshi, MBBS; Lucy E. Kershaw, MSc, PhD; Andy H. Baker² , BSc, PhD; Gerry P. McCann, MBChB, MD; Dana K. Dawson³ , MD, DPhil; Marc R. Dweck⁴ , MBChB, PhD; Scott I. Semple, MSc, PhD;* David E. Newby⁵ , DM, PhD*

BACKGROUND: Takotsubo syndrome is an acute cardiac emergency characterized by transient left ventricular systolic dysfunction typically following a stressful event. Despite its rapidly rising incidence, its pathophysiology remains poorly understood. Takotsubo syndrome may pass unrecognized, especially if timely diagnostic imaging is not performed. Defective myocardial calcium homeostasis is a central cause of contractile dysfunction and has not been explored in takotsubo syndrome. We aimed to investigate myocardial calcium handling using manganese-enhanced magnetic resonance imaging during the acute and recovery phases of takotsubo syndrome.

METHODS: Twenty patients with takotsubo syndrome (63±12 years of age; 90% female) and 20 volunteers matched on age, sex, and cardiovascular risk factors (59±11 years of age; 70% female) were recruited from the Edinburgh Heart Centre between March 2020 and October 2021. Patients underwent gadolinium and manganese-enhanced magnetic resonance imaging during index hospitalization with repeat manganese-enhanced magnetic resonance imaging performed after at least 3 months.

RESULTS: Compared with matched control volunteers, patients had a reduced left ventricular ejection fraction (51±11 versus 67±8%; $P<0.001$), increased left ventricular mass (86±11 versus 57±14 g/m²; $P<0.001$), and, in affected myocardial segments, elevated native T1 (1358±49 versus 1211±28 ms; $P<0.001$) and T2 (60±7 versus 38±3 ms; $P<0.0001$) values at their index presentation. During manganese-enhanced imaging, kinetic modeling demonstrated a substantial reduction in myocardial manganese uptake (5.1±0.5 versus 8.2±1.1 mL/[100 g of tissue ·min], respectively; $P<0.0001$), consistent with markedly abnormal myocardial calcium handling. After recovery, left ejection fraction, left ventricular mass, and T2 values were comparable with those of matched control volunteers. Despite this, native and postmanganese T1 and myocardial manganese uptake remained abnormal compared with matched control volunteers (6.6±0.5 versus 8.2±1.1 mL/[100 g of tissue ·min]; $P<0.0001$).

CONCLUSIONS: In patients with takotsubo syndrome, there is a profound perturbation of myocardial manganese uptake, which is most marked in the acute phase but persists for at least 3 months despite apparent restoration of normal left ventricular ejection fraction and resolution of myocardial edema, suggesting abnormal myocardial calcium handling may be implicated in the pathophysiology of takotsubo syndrome. Manganese-enhanced magnetic resonance imaging has major potential to assist in the diagnosis, characterization, and risk stratification of patients with takotsubo syndrome.

REGISTRATION: URL: <https://www.clinicaltrials.gov>; Unique identifier: NCT04623788.

Key Words: calcium ■ magnetic resonance imaging ■ manganese ■ takotsubo cardiomyopathy

Correspondence to: Trisha Singh, BM, University of Edinburgh, Room SU 305, Chancellor's Building, 49 Little France Crescent, Edinburgh, EH16 4SB, UK. Email tsingh@ed.ac.uk

*S.I. Semple and D.E. Newby contributed equally.

Supplemental Material, the podcast, and transcript are available with this article at <https://www.ahajournals.org/doi/suppl/10.1161/CIRCULATIONAHA.122.060375>.

For Sources of Funding and Disclosures, see page 1834.

Continuing medical education (CME) credit is available for this article. Go to <http://cme.ahajournals.org> to take the quiz.

© 2022 The Authors. *Circulation* is published on behalf of the American Heart Association, Inc., by Wolters Kluwer Health, Inc. This is an open access article under the terms of the [Creative Commons Attribution Non-Commercial License](https://creativecommons.org/licenses/by-nc/4.0/), which permits use, distribution, and reproduction in any medium, provided that the original work is properly cited and is not used for commercial purposes.

Circulation is available at www.ahajournals.org/journal/circ

Clinical Perspective

What Is New?

- In patients with takotsubo syndrome, characteristic patterns of myocardial manganese enhancement can be demonstrated on magnetic resonance imaging.
- Patients with takotsubo syndrome have both acute and persistently abnormal myocardial manganese uptake consistent with underlying abnormalities of myocardial calcium handling.
- Despite apparent restoration of normal systolic function, abnormalities of myocardial calcium handling persist for at least 3 months.

What Are the Clinical Implications?

- Manganese-enhanced magnetic resonance imaging has the potential to diagnose and to characterize takotsubo syndrome even after apparent restoration of normal cardiac function.
- Abnormal myocardial calcium handling as demonstrated by reduced manganese uptake may underlie the pathophysiology of takotsubo syndrome and manganese-enhanced magnetic resonance imaging potentially provides a measure of disease severity.
- Persistent abnormalities of myocardial calcium handling may explain the associated long-term morbidity and mortality of takotsubo syndrome.

Nonstandard Abbreviations and Acronyms

CMR	cardiac magnetic resonance imaging
EF	ejection fraction
MEMORY	Manganese-Enhanced Magnetic Resonance Imaging in Ischaemic, Inflammatory and Takotsubo Cardiomyopathy
MRI	magnetic resonance imaging

Takotsubo syndrome is an acute cardiac emergency that is often triggered by a stressful event and is characterized by transient and profound left ventricular systolic dysfunction, typically attributable to marked ballooning of the left ventricular apex.^{1–3} The pathology of this condition is poorly understood and targeted treatments are lacking. Moreover, recognizing takotsubo syndrome can be challenging because of its phenotypical similarities with acute myocardial infarction; takotsubo syndrome is often considered when invasive coronary angiography fails to identify major obstructive coronary artery disease.⁴ However, the characteristic left ventricular abnormalities can be brief, and opportunities to document them with diagnostic imaging are often missed.⁵

Cardiac magnetic resonance imaging (CMR) is an essential diagnostic tool in the assessment of takotsubo syndrome. In addition to visualizing the hallmark regional wall motion abnormalities, it can identify complications, such as left ventricular outflow tract obstruction, mitral regurgitation, pericardial effusion, and left ventricular thrombus. CMR is particularly useful in establishing the diagnosis of acute cardiac conditions of uncertain origin, such as myocardial infarction with nonobstructive coronary arteries and myocarditis. Previous CMR studies have demonstrated the presence of acute myocardial edema in patients with takotsubo syndrome as well as some reports of persistent subtle cardiac abnormalities after recovery of normal left ventricular ejection fraction.⁶ However, there is a need to develop more sensitive and discriminatory imaging techniques that are less time-sensitive and more specific to takotsubo syndrome.

Manganese, a calcium ion analogue, has paramagnetic properties and can cross intact cell membranes by means of voltage-gated calcium channels, providing intracellular contrast of viable tissue on magnetic resonance imaging (MRI). In 1981, Hunter et al⁷ proposed that uptake of free manganese ions in the myocardium can be used to measure calcium uptake because manganese is retained intracellularly. Manganese-enhanced magnetic MRI thus represents a promising novel approach to the assessment of myocardial calcium handling. We have previously demonstrated differences in manganese uptake in patients with dilated, hypertrophic, or ischemic cardiomyopathy, suggesting abnormal myocardial calcium handling.^{8,9} However, there have been no studies assessing whether manganese-enhanced MRI can detect alterations in myocardial calcium handling in takotsubo syndrome and whether this recovers during convalescence. The objectives of this proof-of-concept study were to evaluate the ability of manganese-enhanced MRI to detect altered myocardial calcium handling in patients with takotsubo syndrome during both the acute presentation and following apparent recovery.

METHODS

MEMORY (Manganese-Enhanced Magnetic Resonance Imaging in Ischaemic, Inflammatory and Takotsubo Cardiomyopathy) was a single-center case-control observational longitudinal cohort study (URL: <https://www.clinicaltrials.gov>; Unique identifier: NCT04623788) conducted in accordance with the Declaration of Helsinki, favorable ethical review of the Southeast Scotland Research Ethics Committee 2 (20/SS/0001), and written informed consent from all participants. The data, analytic methods, and study materials will be made available to other researchers on reasonable request.

Study Populations

Adult patients (≥18 years of age) with takotsubo syndrome were recruited from the Edinburgh Heart Centre between March 2020 and October 2021. Diagnosis of takotsubo syndrome was on the basis of Mayo Clinic and Taskforce on

Takotsubo Syndrome of the Heart Failure Association of the European Society of Cardiology criteria,^{10,11} which comprise new ECG changes (ST-segment elevation, ST-segment depression, T-wave inversion, and QTc prolongation), the presence of transient left ventricular dysfunction presenting as apical ballooning or focal midventricular/basal wall motion abnormalities, and the absence of obstructive coronary artery disease or acute plaque rupture. Patients usually have an emotionally or physically stressful trigger. We specifically excluded patients with pheochromocytoma, myocarditis, or a primary isolated diagnosis of acute myocardial infarction.

Control volunteers were selected consecutively and were matched to patients with takotsubo syndrome 1:1, for age, sex, and cardiovascular risk factor profile, such as hypertension, known coronary artery disease, hypercholesterolemia, and diabetes. All participants were scanned at the University of Edinburgh between September 2020 and August 2021.

Exclusion criteria for all participants were any contraindication to MRI, contraindications to manganese dipyridoxyl diphosphate administration (eg, high-degree atrioventricular block, history of torsades de pointes or prolonged QTc interval, obstructive liver disease), ongoing calcium channel antagonist or digoxin therapy, renal failure (ie, estimated glomerular filtration rate <30 mL/[min·1.73 m²]), New York Heart Association class IV heart failure, and women of childbearing potential without a negative pregnancy test. Participants receiving a calcium channel antagonist had their medication withheld for 48 hours before manganese-enhanced imaging.

Magnetic Resonance Imaging

MRI was performed using a 3T scanner (MAGNETOM Skyrafit; Siemens Healthineers) using a 30-channel anterior body matrix coil and elements of a posterior spine matrix coil. Images were acquired during expiratory breath hold with ECG gating. Cine imaging was acquired with standard steady-state free precession sequences in long- and short-axis orientations as described previously.^{8,9,12} All study participants underwent scanning with both late gadolinium enhancement and manganese-enhanced MRI at least 48 hours apart. Where possible, gadolinium imaging was performed first, with at least 48 hours between the 2 scans (Figure 1).

T1 mapping was performed prospectively with modified Look-Locker inversion (MyoMaps) recovery (repetition time, 388.8 ms; echo time, 1.07 ms; matrix, 256×115; slice thickness, 8 mm with 1.6-mm gap; field of view, 360×288 mm; sampling pattern, 5[3]3). Quantitative estimation of T1 was performed in full short-axis stack from mitral valve annulus to apex and standard long-axis slices, with additional slices positioned appropriately to characterize pathology.

T2 mapping was performed with T2 MyoMaps (repetition time, 207.39 ms; echo time, 1.32 ms; matrix, 192×100; slice thickness, 8 mm with 1.6 mm gap) with T2 evolution times of 0, 0.30, and 0.55 ms. Field of view was 360×288 mm adjusted for patient body habitus as required (MyoMaps; Siemens Healthineers). This was acquired in long-axis and short-axis orientation covering the entire left ventricle.

Late Gadolinium Enhancement

Late gadolinium enhancement images were acquired after intravenous administration of gadobutrol (0.1 mmol/kg;

Gadovist) using a single breath-held phase-sensitive inversion recovery short-axis stack and long-axis orientations (repetition time, 820 ms; echo time, 1.04 ms; matrix, 192×81; slice thickness, 8 mm with 1.8-mm gap; field of view, 380 mm). A standardized inversion time of 400 ms was used and adjusted as required for optimal myocardial nulling. Postcontrast T1 mapping was performed prospectively with short-axis modified Look-Locker inversion recovery stack 10 minutes after contrast administration.

Manganese-Enhanced MRI

Manganese-enhanced MRI was achieved using intravenous infusion of manganese dipyridoxyl diphosphate (5 μmol/kg, 0.1 mL/kg, up to a maximum of 10 mL, 1 mL/min; Exova SL Pharma). T1 mapping was performed precontrast with full short-axis modified Look-Locker inversion recovery stack as above. For patients, a single short-axis slice of the diseased myocardium was identified by the supervising cardiologist and guided by native T1 and T2 maps and cine images (midventricular or basal in all patients). Single short-axis T1 mapping was then performed at this slice location every 2.5 minutes for 30 minutes after beginning contrast infusion. At 30 minutes, a full short-axis T1 stack was repeated (Figure S1). For controls, a midventricular slice was chosen for serial T1 mapping after manganese dipyridoxyl diphosphate infusion.

Image Analysis

All analyses of T1 and T2 maps, late gadolinium enhancement, and cine-derived volumetric and functional sequences were performed using Circle CVI (CVI42 version 5.3.6; Circle Cardiovascular Imaging) as previously validated and described in animal and human models.^{8,9,13} Image analysis was conducted blind to patient details (analyzed in groups after the end of the scanning period) and manganese-enhanced images were analyzed separately from late gadolinium images. Endocardial and epicardial borders were defined manually on all conventional short-axis images for volumetric and wall motion measurements and were then copied to corresponding T1 map images for analysis with minimal manual adjustments. The left ventricular basal short-axis slice was identified as the image containing at least 50% of circumferential myocardium at end diastole. Papillary muscles were included in the mass and excluded from volumetric analysis.

After contouring, an additional epicardial and endocardial offset of 20% was applied automatically to minimize partial volume effect for all T1 map analyses. In patients, T1 and T2 measurements were taken from septal segments in both pathologic (area with regional wall motion abnormality) and remote regions (no regional wall motion abnormality). In control volunteers, T1 and T2 measurements were made in the septal wall of the midventricular slice (Figure S2). Global native and postmanganese T1 and Ki (mean of 6 segments from a short-axis slice) were also measured in patients (excluding focal takotsubo and dual pathology; n=4) and volunteers (Table S1). Left ventricular wall thickness was measured in the pathologic and remote myocardium (septal walls for both) for acute and follow-up scans. For matched volunteers, wall thickness was measured in the midventricular septal wall (Figure S3).

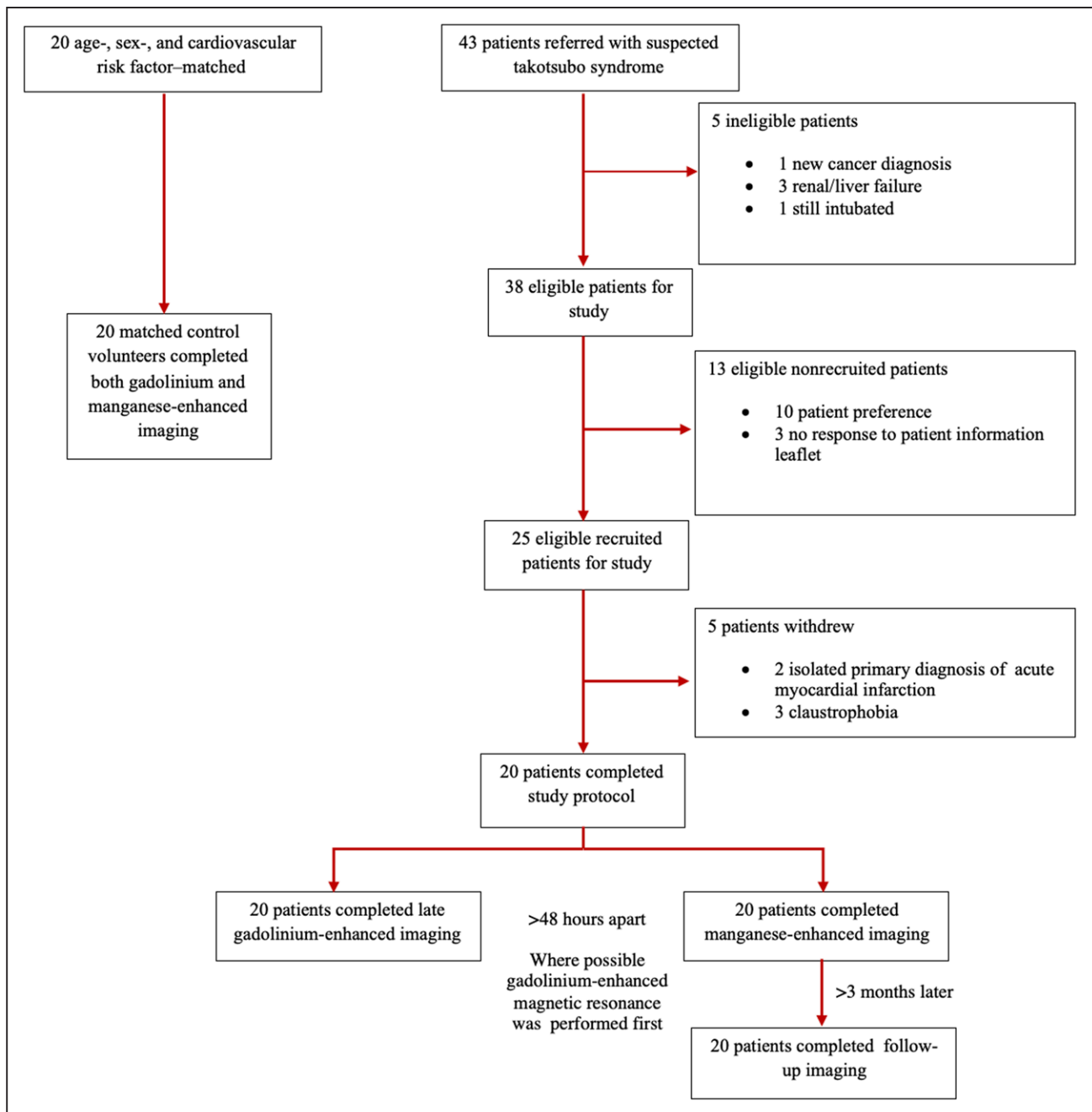


Figure 1. Consort diagram.

Manganese Kinetic Modeling

Manganese uptake was calculated for a selected single short-axis slice of the diseased myocardium, which was chosen on the basis of the presence of regional wall motion abnormality, and native T1 and T2 maps. To quantify the change in T1 over time, regions of interest were drawn as described previously. For postmanganese serial T1 imaging, manually drawn regions of interest from the precontrast image were transferred to all subsequent postcontrast images to ensure consistency. The rate of myocardial manganese uptake (Ki) was determined by Patlak modeling, as described previously.^{12,14,15}

Statistical Analysis

All statistical analysis was performed with GraphPad Prism (version 8.0.2; GraphPad Software). Categorical baseline variables were presented as number (%) and compared using χ^2 test. Continuous data were assessed for normality using the D'Agostino-Pearson test and presented as mean \pm SD or median (interquartile interval). Cardiac function, myocardial manganese uptake, volumetric assessment, and parametric mapping values were compared using paired Student *t* tests and Wilcoxon signed rank and unpaired *t* test or Mann-Whitney tests where appropriate. Sensitivity analyses were performed excluding the focal subtype of takotsubo syndrome or the presence of dual

Table 1. Baseline Characteristics of the Study Population

Characteristics	Matched controls (n=20)	Patients with takotsubo syndrome (n=20)
Age, y [†]	59 (29–70)	63 (42–80)
Female sex	14 (70)	18 (90)
Body mass index, kg/m ^{2†}	27 (21–35)	25 (22–33)
Past medical history		
Hypertension	7 (35)	8 (40)
Known coronary artery disease	2 (10)	2 (10)
Hypercholesterolemia	5 (25)	5 (25)
Acute neurologic/psychiatric disorder	0	1 (5)
Past chronic neurologic/psychiatric disorder	4 (20)	14 (70)
Depression	3 (15)	7 (35)
Anxiety disorder	1 (5)	6 (30)
Schizophrenia	0	1 (5)
Diabetes	2 (10)	2 (10)
Thyroid disorder	0	2 (10)
Asthma	0	1 (5)
Medications before admission		
Antiplatelet therapy	2 (10)	2 (10)
β-Blocker therapy	2 (10)	2 (10)
ACE inhibitor or ARB therapy	4 (35)	2 (10)
Calcium channel blockers	1 (10)	5 (25)
Statin therapy	5 (25)	5 (25)
Antiglycemic therapy	2 (10)	2 (10)
Previous/current antidepressant therapy	2 (10)	9 (45)
Presenting symptom		
Dyspnea	–	6 (30)
Chest pain	–	14 (70)
Stressor		
Emotional	–	13 (65)
Physical	–	4 (20)
None	–	3 (15)
Peak plasma cardiac high-sensitive troponin I concentration, ng/L	–	6981
ECG		
ST-segment elevation	–	8 (40)
ST-segment depression	–	2 (10)
T-wave changes	–	10 (50)
QTc, ms	387±13	552±42
Index left ventricular ejection fraction		
Borderline (50%–54%)	–	4 (20)
Impaired (36%–49%)	–	9 (45)
Severely impaired (<35%)	–	7 (35)
Coronary angiography		
Normal coronaries	–	10 (50)

(Continued)

Table 1. Continued

Characteristics	Matched controls (n=20)	Patients with takotsubo syndrome (n=20)
Nonobstructive arteries	–	10 (50)
Obstructive disease	–	0
Left ventriculography completed	–	13 (65)
Takotsubo syndrome subtype		
Apical	–	17 (85)
Basal	–	1 (5)
Focal	–	2 (10)
Treatment initiated/stopped		
Antiplatelet therapy	–	10 (50)
β-Blocker therapy	–	18 (90)
Angiotensin-converting enzyme inhibitor or angiotensin receptor blocker therapy	–	16 (80)
Diuretic therapy	–	6 (30)
Statin therapy	–	5 (25)
Calcium channel antagonist [‡]	1 (10)	5 (25)
Days since acute episode	–	100 (87–368)
Symptoms at follow-up		
Chest pain	–	0 (0)
Dyspnea	–	5 (28)
Palpitations	–	2 (11)
Fatigue	–	4 (20)
Adverse events at follow-up		
Cerebrovascular event	–	1 (5)
Reoccurrence	–	1 (5)
Death	–	0 (0)

Values are n (%), median (interquartile range), or mean±SD.

**P*≤0.1.†*P*≤0.67.

‡Withdrawn at presentation in patients or for at least 48 hours before manganese-enhanced magnetic resonance imaging.

pathology. Correlations were assessed using linear regression analysis. Statistical significance was taken as 2-sided *P*<0.05.

RESULTS

Study Populations

Twenty-five patients with takotsubo syndrome were recruited into the study and 5 were withdrawn (3 were unable to complete the cardiac magnetic resonance scan because of claustrophobia and 2 had an infarct pattern of late gadolinium enhancement on MRI and an isolated primary diagnosis of acute myocardial infarction; Figure 1). The patient cohort was predominantly middle-aged women (Table 1). All patients had symptoms (chest pain in 70% and dyspnea in 30%) requiring emergency hospitalization with the majority having an identifiable precipitating stressor (Table S2). Only 2 patients

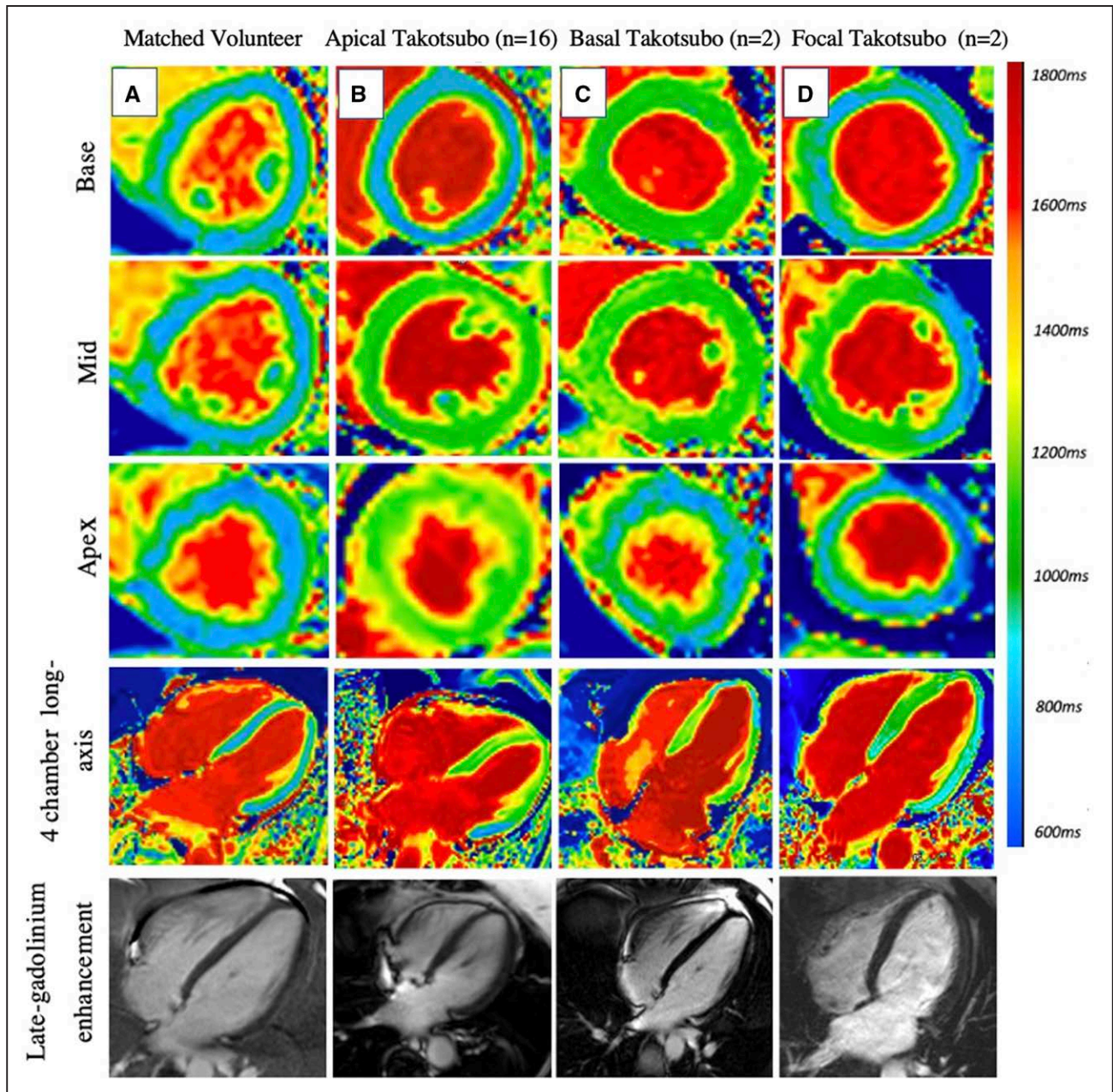


Figure 2. Anatomic types of takotsubo syndrome.

Short-axis and long-axis manganese-enhanced T1 maps and long-axis late gadolinium images (10 minutes postcontrast) in a matched control volunteer (A) and patients with apical (B), basal (C), or focal (D) takotsubo syndrome. Blue represents normal manganese uptake and green represents reduced manganese uptake and abnormal calcium handling.

had preexisting symptoms (1 chest pain, 1 palpitation). Twenty control volunteers were well-matched for age and comorbidities although there was a higher prevalence of women and preexisting psychiatric or neurologic disorders in the patient cohort (Table 1). There were no demonstrable differences in myocardial manganese uptake according to the use of antidepressant therapies (Table S3). We found no difference in myocardial manganese uptake in our control cohort between women and men (8.2 ± 0.7 versus 8.3 ± 1.0 mL/[100 g of tissue·min]; $P=0.71$). Five patients and 1 control volunteer previously

were taking calcium channel antagonists. All patients had this therapy discontinued at presentation because of the presence of left ventricular dysfunction and the control volunteer had the calcium channel antagonist withheld 48 hours before manganese-enhanced MRI.

Manganese Infusion

Sixty infusions of manganese dipyridoxyl diphosphate were completed during the course of the study (mean duration of 10 minutes). There were

no changes in ECG, heart rate, or blood pressure (Figure S4) after manganese administration ($P>0.1$ for all). One healthy volunteer experienced mild transient nausea for <10 seconds after commencing manganese infusion, which resolved spontaneously without intervention. Otherwise, contrast administration was well-tolerated with no adverse reactions reported during or immediately after administration or at follow-up at 7 days.

Characterization of Takotsubo Syndrome

ECG demonstrated either ST-segment deviation or T-wave changes in all patients, with evidence of QT interval prolongation in some patients. All patients had a degree of left ventricular impairment on baseline echocardiographic imaging. All patients underwent invasive coronary angiography, which demonstrated normal coronary arteries in half of the population, with the remaining having nonobstructive coronary artery disease (Table 1 and Table S4). Two patients had evidence of acute coronary pathology: 1 had spontaneous coronary artery dissection in the first obtuse marginal and

the second had plaque rupture in the distal left anterior or descending artery. In both cases, coronary flow had been restored and there were extensive regional wall motion abnormalities involving all midventricular and apical segments that were not in keeping with myocardial infarction alone. Most patients had an apical pattern of takotsubo syndrome (Figure 2). Two patients demonstrated a focal pattern of takotsubo syndrome: 1 had normal coronary arteries and the other had mild plaque in the left anterior descending artery and underwent intracoronary imaging (demonstrated stable plaque) and a pressure wire study (fractional flow reserve during maximal hyperemia, 0.92). Both patients demonstrated rapidly resolving left ventricular function and had no evidence of late gadolinium enhancement. On discharge, all patients began heart failure treatment, with a smaller proportion being started on diuretic therapy. Patients who had evidence of coronary artery disease began antiplatelet therapy and 2 patients were started on dual antiplatelet therapy (Table 1). During follow-up, 1 patient had a stroke and another had recurrence of takotsubo syndrome within a year of the index event.

Table 2. Cardiac Magnetic Resonance Findings

Variable	Matched controls (n=20)	Patients with takotsubo syndrome: index event (n=20)	Patients with takotsubo syndrome: follow-up (n=20)	P value*	P value†
Time between symptom onset and scan, median, d	–	4 (1–18)	100 (87–368)		
Left ventricular end-diastolic volume index, mL/m ²	79±15	71±20	72±11	0.1	0.09
Left ventricular end-systolic volume index, mL/m ²	27±7	36±11	23±9	0.03‡	0.89
Stroke volume index, mL/m ²	51±11	39±12	46±7	0.002‡	0.83
Left ventricular ejection fraction, %	67±8	51±11	69±4	<0.001‡	0.61
Left ventricular mass index, g/m ²	57±14	86±11	55±13	<0.001‡	0.71
Left ventricular wall thickness—pathologic, mm	7.0±0.9	13.1±1.5	7.3±1.3	<0.001‡	0.12
Left ventricular wall thickness—remote, mm	6.9±0.9	10.4±1.8	7.0±1.1	<0.001‡	0.09
Right ventricular ejection fraction, %	63±6	63±10	66±4	0.47	0.09
Global longitudinal strain, %	–18±1	–12±6	–16±3	0.003‡	0.09
Late gadolinium enhancement pattern	0 (0)	2 (10)	–		
Ischemic	–	2 (10)	–		
Native T1 in pathologic segment, ms	1211±28	1358±49	1238±35	<0.0001‡	0.02‡
Native T1 in remote segment, ms	1211±28	1255±56	1209±27	0.01‡	0.84
Native T2 in pathologic segment, ms	38±3	60±7	39±2	<0.0001‡	0.12
Native T2 in remote segment, ms	38±3	43±5	36±3	0.002‡	0.24
Global extracellular volume, %	26±3	34±5	–	<0.0001‡	–
Myocardial T1 30 minutes after manganese pathologic segment, ms	884±26	1030±48	919±31	<0.0001‡	0.003‡
Myocardial T1 30 minutes after manganese remote segment, ms	884±26	920±16	900±9	<0.0001‡	0.002‡
Manganese influx, Ki, mL/100 g of tissue, min	8.2±1.1	5.1±0.5	6.6±0.5	<0.0001‡	<0.0001‡

Values are n (%), median (interquartile range), or mean±SD.

*Controls versus patients with takotsubo syndrome at index presentation.

†Controls versus patients with takotsubo syndrome at follow-up.

‡Significant.

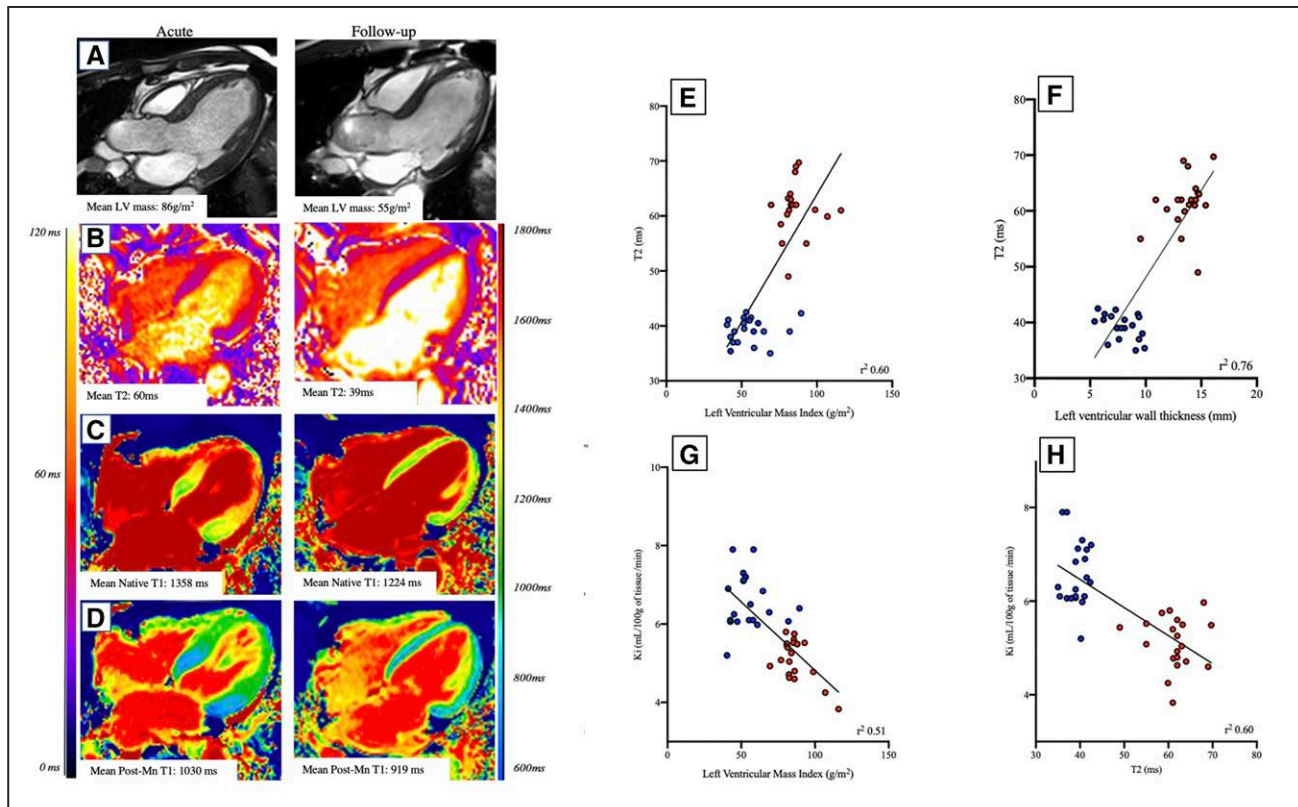


Figure 3. Myocardial edema and left ventricular mass in takotsubo syndrome.

Changes in left ventricular (LV) mass (A), native T2 (B), native T1 (C), and 30-minute postmanganese T1 maps (D). Correlations are seen between LV mass and native T2 (E), left ventricular wall thickness and native T2 (F), myocardial manganese uptake and LV mass (G), and myocardial manganese uptake and native T2 (H) during acute (red) and follow-up (blue) scans.

Magnetic Resonance Imaging

Acute Index Presentation

Most patients underwent CMR within a median of 4 days (range, 1 to 18 days) of symptom onset. Compared with matched control volunteers, patients with takotsubo syndrome had reduced left ventricular ejection fraction (Table 2), increased left ventricular mass (Figure 3), and comparable right ventricular systolic function. Left ventricular wall thickness was elevated in pathologic and remote regions (Table 2). Two patients had late gadolinium enhancement consistent with acute myocardial infarction (dual pathology; Figure 4). Two patients demonstrated hazy incomplete nulling of late gadolinium enhancement imaging in midventricular and apical segments consistent with the marked characteristic edema of takotsubo syndrome (Figure 4).

Compared with matched control volunteers, patients with takotsubo syndrome had elevated native T1 and T2 values in both the pathologic and remote myocardial segments (Table 2). After manganese infusion, T1 shortening was less pronounced in patients with takotsubo syndrome (Table 2), with kinetic modeling demonstrating marked reductions in myocardial manganese uptake in the pathologic myocardium (5.1 ± 0.5 versus 8.2 ± 1.1 mL/[100 g of tissue·min]; $P < 0.0001$). Segments with

reduced myocardial manganese uptake corresponded with areas of myocardial edema and regional wall motion abnormalities. Subgroup analysis with the exclusion of the focal subtype of takotsubo syndrome ($n=2$; Table S5) or dual pathology ($n=2$; Table S6) demonstrated findings consistent with the entire cohort.

One patient underwent CMR 18 days after the onset of presentation symptoms and there was complete resolution of regional wall motion abnormalities and normal left ventricular systolic function. Despite this, manganese-enhanced T1 mapping demonstrated a pattern of reduced myocardial manganese uptake consistent with apical takotsubo syndrome (Figure 5).

Follow-Up at 3 Months

All 20 patients returned for follow-up and underwent repeat manganese-enhanced MRI a median of 100 days (range, 87 to 368) after symptom onset (Table 2), with 11 (65%) patients describing ongoing symptoms (Table 1). There was restoration of normal left ventricular ejection fraction and resolution of regional wall motion abnormalities in almost all patients (Table 2). Of the patients who were diagnosed with dual pathology ($n=2$), 1 demonstrated hypokinesis in the inferior wall despite normalization of left ventricular ejection fraction (acute myocardial infarction and takotsubo

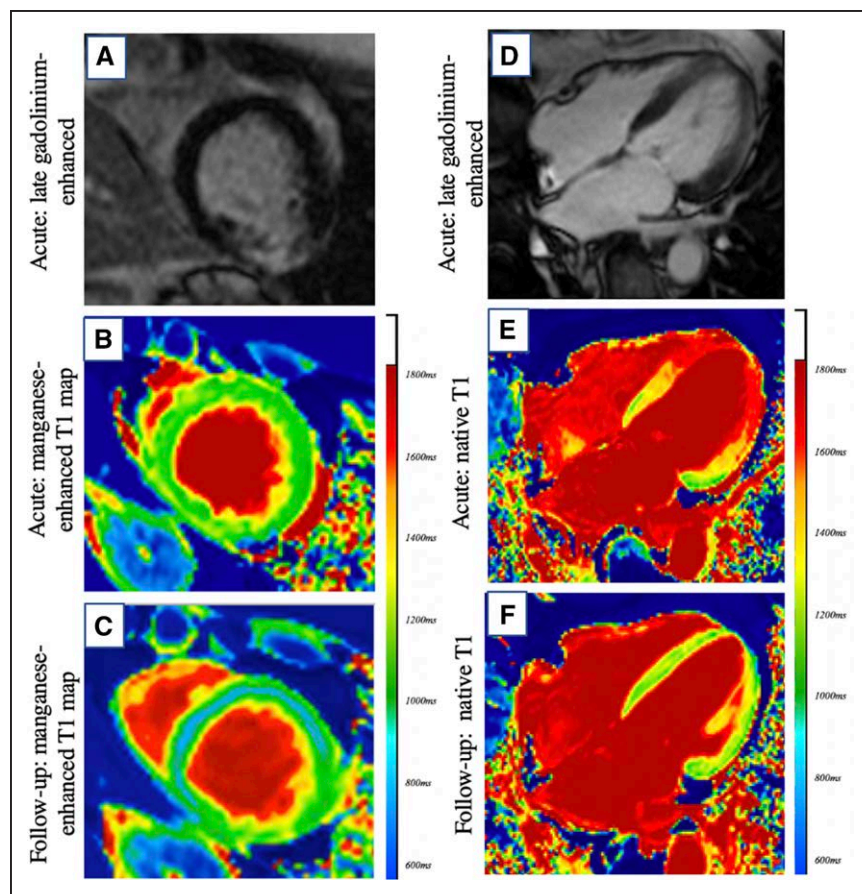


Figure 4. Gadolinium enhancement in patients with takotsubo syndrome.

Short-axis views of inferior late gadolinium enhancement in a patient with spontaneous coronary artery dissection of the obtuse marginal branch of the left circumflex artery (A) and apical takotsubo (dual pathology). (B) During acute imaging, reduced myocardial manganese uptake (green) extends beyond the infarct region. (C) Follow-up imaging demonstrating recovery of manganese uptake (blue) in regions affected by takotsubo syndrome with persistent abnormal manganese uptake (green) in the infarct region. (D) Long-axis, 4-chamber view demonstrating characteristic hazy “incomplete nulling” in late gadolinium enhancement imaging in a patient with apical takotsubo. (E) Corresponding native T1 map during acute event demonstrating elevated native T1 in midventricle and apical segments, with resolution on follow-up scans (F).

syndrome) and the other had resolution of the regional wall motion abnormality.

In patients with takotsubo syndrome, native and post-manganese T1 values were reduced compared with those obtained after the acute index event but remained higher than the matched control volunteers ($P=0.02$ and $P=0.003$, respectively). T2 values in the previously pathologic myocardium normalized and were comparable to those of matched control volunteers ($P=0.12$). Left ventricular mass and left ventricular wall thickness (pathologic and remote) were also reduced and correlated with the reduction in myocardial native T2 values ($r^2=0.6$ and 0.7 , respectively; Figure 3). Myocardial manganese uptake demonstrated some improvement but remained persistently abnormal at follow-up (Table 2 and Figure 6). Manganese uptake correlated with improvement in left ventricular mass and T2 values (Figure 3). Subgroup analysis with the exclusion of the focal subtype of takotsubo syndrome ($n=2$; Table S5) or dual pathology ($n=2$; Table S6) demonstrated consistent findings.

DISCUSSION

We provide the first description of manganese-enhanced MRI in detecting abnormal myocardial cellular physiology in patients with takotsubo syndrome. Our findings demonstrate that there is a profound disturbance in manga-

nese uptake indicative of abnormal myocardial calcium handling. This is most marked in the acute setting but remains abnormal after apparent recovery of left ventricular function. This abnormal myocardial calcium handling may contribute to the underlying pathophysiology of this condition and perhaps explains persistent symptoms reported by some patients and the high rate of recurrence of takotsubo syndrome.^{16–19}

For the first time, we have demonstrated a profound in vivo abnormality of myocardial calcium handling in patients with takotsubo syndrome. Our findings support previously described abnormalities of intracellular calcium handling in endomyocardial biopsies obtained from patients with takotsubo syndrome and acute left ventricular dysfunction.²⁰ Here, calcium-regulating proteins, such as phospholamban, SERCA (sarcoendoplasmic reticulum calcium-adenosine triphosphatase), and sarcolipin, were markedly altered, suggesting that this may be responsible for the associated ventricular dysfunction. Using myocardial manganese uptake as a measure of the flux of intracellular calcium ions, we confirm that marked alterations in myocardial calcium handling appear to play a major pathophysiologic role in takotsubo syndrome, especially in the acute high-risk period. Such a mechanism could explain why levosimendan can improve cardiogenic shock during acute severe cases of takotsubo syndrome, because it augments

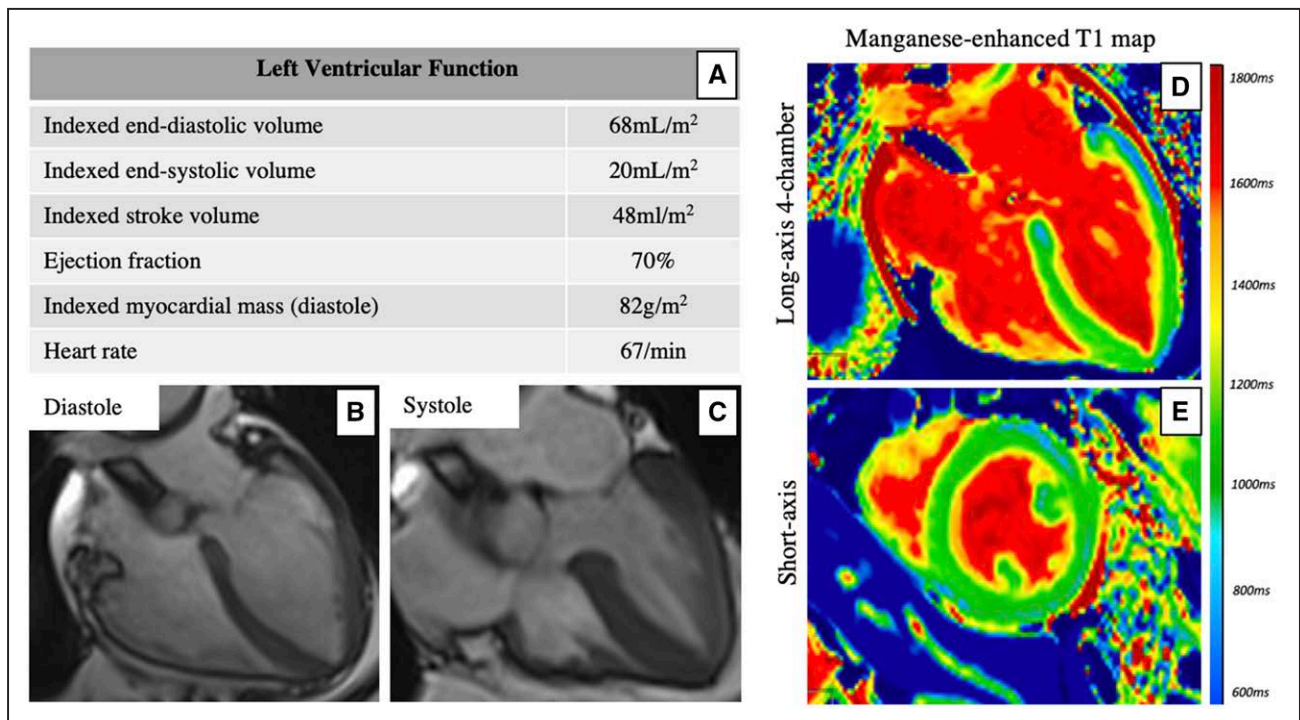


Figure 5. Manganese-enhanced magnetic resonance imaging in takotsubo syndrome.

Resolution of left ventricular systolic dysfunction (**A**) and apical ballooning (**B** and **C**) in a patient with takotsubo syndrome scanned 18 days after symptom onset. (**D**) Long-axis and (**E**) short-axis manganese-enhanced T1 map demonstrating typical apical pattern of takotsubo syndrome with abnormal myocardial manganese uptake (green) in midventricular and apical segments with normal uptake (blue) in basal segments despite apparent restoration of normal cardiac function.

myocardial calcium binding to troponin C. Although this is an important fundamental mechanistic observation, we cannot determine whether these alterations are a consequence or a cause of the takotsubo syndrome and this will require further study.

Takotsubo syndrome is partly defined by the apparent dramatic improvement of left ventricular function after the acute dramatic emergent presentation. The rapid transition from severe left ventricular systolic dysfunction and low ejection fraction to apparently normal left ventricular function and ejection fraction within days is a characteristic feature of this condition. However, this can create challenges for the diagnosis of this condition, because unless the index of suspicion is high and the diagnosis is considered early, these typical features will resolve and the opportunity to undertake diagnostic imaging may have passed. In this regard, manganese-enhanced MRI may provide an opportunity to identify the typical distribution of myocardial abnormalities despite normalization of regional wall motion abnormalities. This provides a unique opportunity to diagnose this condition at later time points and help resolve potential diagnostic uncertainties especially where the clinical suspicion of the diagnosis was initially low. There also can be major diagnostic uncertainty in cases of dual pathology, where acute myocardial infarction triggers a takotsubo syndrome, as demonstrated by 2 examples in our case series. Manganese-enhanced MRI could therefore

prove invaluable in identifying and discriminating cases of takotsubo syndrome, especially when the precipitating event is caused by another primary cardiac condition.

There are major implications for the protracted abnormalities in myocardial calcium handling. First, these findings could account for the persistence of symptoms and reduced exercise capacity reported by patients who have apparently recovered from takotsubo syndrome.²¹ The majority of patients continue to complain of fatigue, tiredness, and reduced exercise tolerance despite normal left ventricular ejection fraction. Continued long-term impairment in cardiac energetic status and reduced exercise maximal oxygen capacity has been described previously and are likely to be linked to the abnormalities of myocardial calcium handling.²¹ Indeed, 60% of our cohort described ongoing symptoms at follow-up, compatible with a heart failure-like syndrome with a substantial effect on quality of life.

In contrast with the belief that the heart recovers spontaneously and completely without clinical sequelae, patients with takotsubo syndrome are now recognized to have substantial long-term morbidity and mortality that is comparable to that of acute myocardial infarction.^{16,19,22–25} Long-term rates of cerebrovascular and cardiac events and recurrent takotsubo syndrome approach 10% and 2% per year.^{19,24} We have recently reported abnormal myocardial manganese uptake in patients with dilated or hypertrophic cardiomyopathy as well as those with acute

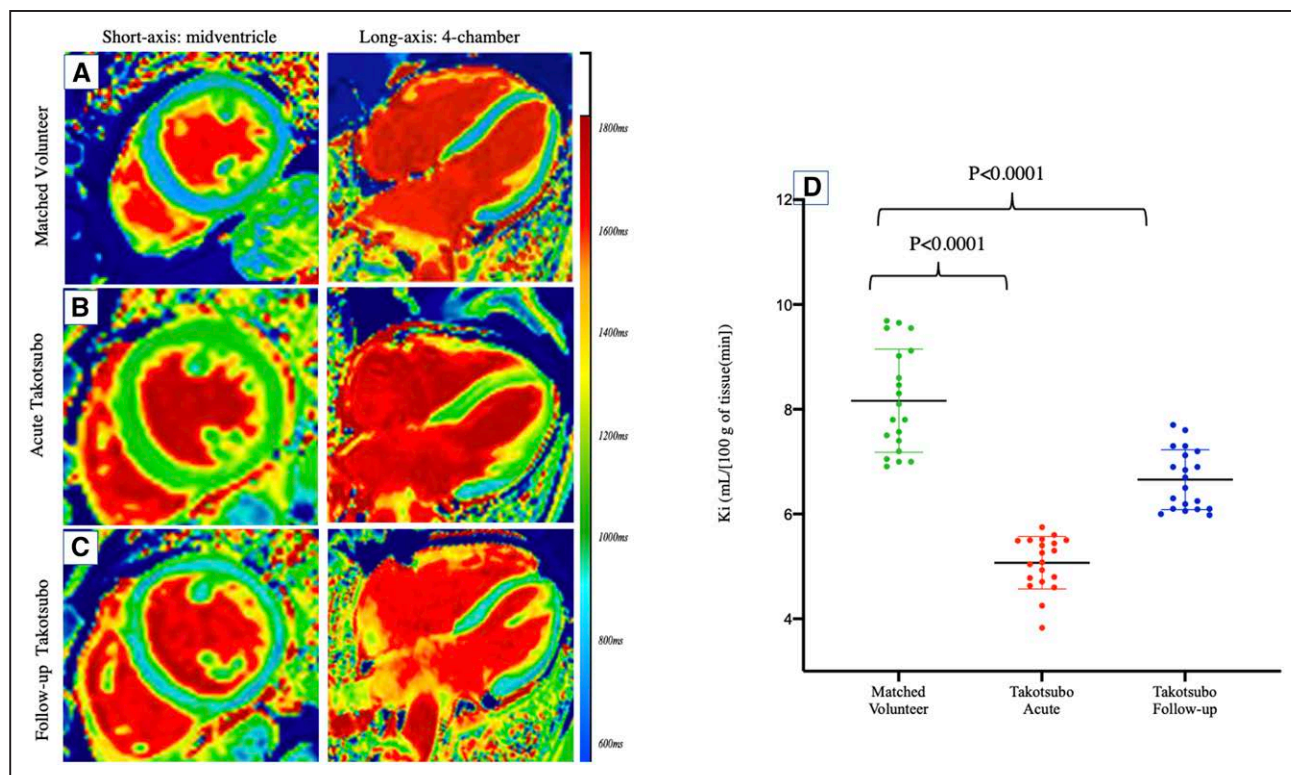


Figure 6. Myocardial calcium handling in takotsubo syndrome.

Short-axis and long-axis manganese-enhanced T1 map in (A) a matched control volunteer and (B) a patient with acute takotsubo syndrome demonstrating reduced manganese uptake (green). Short-axis and long-axis manganese-enhanced T1 maps at follow-up (C) demonstrating improvement (patchy) in myocardial manganese uptake (as calculated by Patlak modeling) but persistent abnormalities compared with matched control volunteers (D).

myocardial infarction.⁹ Levels of myocardial manganese uptake were more impaired in patients who had recovered from takotsubo syndrome than in those with dilated cardiomyopathy despite the latter having more marked left ventricular systolic dysfunction.⁹ Indeed, such was the profound suppression of manganese enhancement during the acute phase of takotsubo syndrome that it was comparable to the infarcted myocardium of patients with acute myocardial infarction and the densely fibrotic regions in the left ventricle of patients with hypertrophic cardiomyopathy.

It would have been ideal to assess patients with takotsubo syndrome before their incident event, but the longer-term persistence of abnormal myocardial calcium handling does suggest an underlying cardiomyopathy that is only brought to light after an acute stressful event. As such, we may never see normalization of myocardial calcium handling, which is in keeping with previous studies describing a heart failure–like phenotype in this patient cohort.²¹

There are potential opportunities for manganese-enhanced MRI to play an important role in prognostication and the assessment of novel treatment interventions. Persistent perturbation of myocardial calcium handling may identify those patients who are at risk of incident or recurrent cases of takotsubo syndrome. Whereas this

would seem intuitive, large prospective patient cohort studies are required to establish whether this is indeed the case. In addition, there are no proven treatments to improve the symptoms and clinical outcomes of patients with takotsubo syndrome. The assessment of myocardial calcium handling using manganese-enhanced MRI could provide a useful surrogate biomarker of treatment efficacy. This is particularly important because standard measures of cardiac function, such as left ventricular ejection fraction, appear to be normal in patients who have recovered from takotsubo syndrome, and this has limited the field in terms of assessing the efficacy of potential preventative therapeutic interventions. It is noteworthy that persistent abnormalities of myocardial calcium handling were present despite the initiation of angiotensin-converting enzyme inhibitor or β -blocker therapies in many of our patients.

Our study has several limitations that should be acknowledged. First, there have been concerns regarding toxicity of unchelated forms of manganese. However, the chelated form of manganese used here retains the necessary properties for intracellular myocardial manganese uptake without any demonstrable adverse hemodynamic or arrhythmic effects.^{26,27} Second, our study population size was modest, although we detected substantial and large abnormalities in myocardial calcium handling.

Future multicenter studies of larger patient populations are needed to demonstrate the robustness, generalizability, and clinical usefulness of our findings in this proof-of-concept study. Third, the Patlak model assumes that perfusion is normal. Whereas we excluded epicardial coronary flow disturbance on invasive angiography in all patients, microvascular impairment and reduced myocardial perfusion may have contributed to reductions in manganese uptake. However, although microvascular impairment is a potential feature in takotsubo syndrome,²⁸ this abnormality improves as myocardial function normalizes,²⁹ and we observed persistent long-term abnormalities of myocardial manganese uptake after apparent recovery. This suggests that microvascular impairment alone is unlikely to be the cause of the marked myocardial manganese abnormality seen in our takotsubo syndrome cohort. Last, no preparations of manganese-based contrast medium are available for widespread clinical use. However, this is likely to change, with commercially available preparations anticipated in the near future.

We have conducted the first proof-of-concept study of manganese-enhanced MRI in patients with takotsubo syndrome. Using kinetic modeling, we have observed dysfunctional myocardial calcium influx in patients with takotsubo syndrome, which is most striking during the acute episode but persists despite improvement of edema and myocardial function. Manganese-enhanced MRI holds major promise for the diagnosis, risk stratification, and monitoring of disease, with the potential for the assessment of novel treatment interventions.

ARTICLE INFORMATION

Received April 8, 2022; accepted September 29, 2022.

Affiliations

BHF/University Centre for Cardiovascular Science (T.S., S.J., L.E.K., A.H.B., M.R.D., S.I.S., D.E.N.) and Edinburgh Imaging (T.S., S.J., L.E.K., A.H.B., M.R.D., S.I.S., D.E.N.), University of Edinburgh, UK. Edinburgh Heart Centre, Royal Infirmary of Edinburgh, United Kingdom (T.S., S.J., A.H.B., M.R.D., D.E.N.). Aberdeen Cardiovascular and Diabetes Centre, University of Aberdeen, United Kingdom (D.K.D.). Department of Cardiovascular Sciences, University of Leicester and NIHR Leicester Biomedical Research Centre, Glenfield Hospital, United Kingdom (G.P.M.).

Acknowledgments

The authors thank the Edinburgh Imaging Facility.

Sources of Funding

This work and T. Singh, S. Joshi, and Drs Dweck and Newby are supported by the British Heart Foundation (grants FS/17/19/32641, CS/17/1/32445, RG/16/10/32375, RE/18/5/34216, FS/ICRF/20/26002, and FS/SCRF/21/32010). T. Singh is supported by the Medical Research Council (grant MR/T029153/1). Dr Newby is the recipient of a Wellcome Trust Senior Investigator Award (WT103782AIA). Dr McCann is supported by an NIHR Research Professorship (08-2017-ST2-007). The Edinburgh Clinical Research Facilities and Edinburgh Imaging Facility are supported by the National Health Service Research Scotland through the National Health Service Lothian Health Board.

Disclosures

Drs Newby and Semple hold unrestricted educational grants from Siemens Healthineers. Dr McCann holds a research agreement with Circle CVI through University Hospitals of Leicester NHS Trust.

Supplemental Material

Expanded Methods

Figures S1–S4

Tables S1–S6

REFERENCES

- Ghadri JR, Wittstein IS, Prasad A, Sharkey S, Dote K, Akashi YJ, Cammann VL, Crea F, Galiuto L, Desmet W, et al. International expert consensus document on takotsubo syndrome (part I): clinical characteristics, diagnostic criteria, and pathophysiology. *Eur Heart J*. 2018;39:2032–2046. doi: 10.1093/eurheartj/ehy076
- Sato H, Tateishi H, Uchida T. *Takotsubo-like left ventricular dysfunction due to multivessel coronary spasm*. In: Clinical Aspect of Myocardial Injury: From Ischemia to Heart Failure. Tokyo, Japan: Kagakuhyoronsha; 1990.
- Akashi YJ, Goldstein DS, Barbaro G, Ueyama T. Takotsubo cardiomyopathy: a new form of acute, reversible heart failure. *Circulation*. 2008;118:2754–2762. doi: 10.1161/CIRCULATIONAHA.108.767012
- Kurusu S, Sato H, Kawagoe T, Ishihara M, Shimatani Y, Nishioka K, Kono Y, Umemura T, Nakamura S. Takotsubo-like left ventricular dysfunction with ST-segment elevation: a novel cardiac syndrome mimicking acute myocardial infarction. *Am Heart J*. 2002;143:448–455. doi: 10.1067/mhj.2002.120403
- Citro R, Okura H, Ghadri JR, Izumi C, Meimoun P, Izumo M, Dawson D, Kaji S, Eitel I, Kagiyama N, et al. Multimodality imaging in takotsubo syndrome: a joint consensus document of the European Association of Cardiovascular Imaging (EACVI) and the Japanese Society of Echocardiography (JSE). *J Echocardiogr*. 2020;18:199–224. doi: 10.1007/s12574-020-00480-y
- Scally C, Abbas H, Ahearn T, Srinivasan J, Mezincescu A, Rudd A, Spath N, Yucel-Finn A, Yucel R, Oldroyd K, et al. Myocardial and systemic inflammation in acute stress-induced (takotsubo) cardiomyopathy. *Circulation*. 2019;139:1581–1592. doi: 10.1161/CIRCULATIONAHA.118.037975
- Hunter DR, Haworth RA, Berkoff HA. Cellular manganese uptake by the isolated perfused rat heart: a probe for the sarcolemma calcium channel. *J Mol Cell Cardiol*. 1981;13:823–832. doi: 10.1016/0022-2828(81)90239-x
- Spath NB, Singh T, Papanastasiou G, Baker A, Janiczek RJ, McCann GP, Dweck MR, Kershaw L, Newby DE, Semple S. Assessment of stunned and viable myocardium using manganese-enhanced MRI. *Open Heart*. 2021;8:e001646. doi: 10.1136/openhrt-2021-001646
- Spath NB, Singh T, Papanastasiou G, Kershaw L, Baker AH, Janiczek RL, Gulsin GS, Dweck MR, McCann G, Newby DE, et al. Manganese-enhanced magnetic resonance imaging in dilated cardiomyopathy and hypertrophic cardiomyopathy [published online November 17, 2020]. *Eur Heart J Cardiovasc Imaging*. doi: 10.1093/ehjci/jeaa273
- Abe Y, Kondo M, Matsuoka R, Araki M, Dohyama K, Tanio H. Assessment of clinical features in transient left ventricular apical ballooning. *J Am Coll Cardiol*. 2003;41:737–742. doi: 10.1016/s0735-1097(02)02925-x
- Maron BJ, Towbin JA, Thiene G, Antzelevitch C, Corrado D, Arnett D, Moss AJ, Seidman CE, Young JB. Contemporary definitions and classification of the cardiomyopathies: an American Heart Association scientific statement from the council on clinical cardiology, heart failure and transplantation committee; quality of care and outcomes research and functional genomics and translational biology interdisciplinary working groups; and council on epidemiology and prevention. *Circulation*. 2006;113:1807–1816. doi: 10.1161/CIRCULATIONAHA.106.174287
- Singh T, Kite TA, Joshi SS, Spath NB, Kershaw L, Baker A, Jordan H, Gulsin GS, Williams MC, van Beek EJR, et al. MRI and CT coronary angiography in survivors of COVID-19. *Heart*. 2022;108:46–53. doi: 10.1136/heartjnl-2021-319926
- Spath N, Tavares A, Gray GA, Baker AH, Lennen RJ, Alcaide-Corral CJ, Dweck MR, Newby DE, Yang PC, Jansen MA, et al. Manganese-enhanced t1 mapping to quantify myocardial viability: validation with (18)f-fluorodeoxyglucose positron emission tomography. *Sci Rep*. 2020;10:2018. doi: 10.1038/s41598-020-58716-x
- Patlak CS, Blasberg RG, Fenstermacher JD. Graphical evaluation of blood-to-brain transfer constants from multiple-time uptake data. *J Cereb Blood Flow Metab*. 1983;3:1–7. doi: 10.1038/jcbfm.1983.1
- Skjold A, Kristoffersen A, Vangberg TR, Haraldseth O, Jynge P, Larsson HB. An apparent unidirectional influx constant for manganese as a measure of myocardial calcium channel activity. *J Magn Reson Imaging*. 2006;24:1047–1055. doi: 10.1002/jmri.20736
- Singh T, Khan H, Gamble DT, Scally C, Newby DE, Dawson D. Takotsubo syndrome: Pathophysiology, emerging concepts, and clinical implications.

- Circulation*. 2022;145:1002–1019. doi: 10.1161/CIRCULATIONAHA.121.055854
17. El-Batrawy I, Gietzen T, Ansari U, Behnes M, Lang S, Zhou X, Borggrete M, Akin I. Short-term and long-term incidence of stroke in takotsubo syndrome. *ESC Heart Fail*. 2018;5:1191–1194. doi: 10.1002/ehf2.12357
 18. El-Batrawy I, Gietzen T, Lang S, Ansari U, Behnes M, Zhou X, Borggrete M, Akin I. Short- and long-term incidence of thromboembolic events in takotsubo syndrome as compared with acute coronary syndrome. *Angiology*. 2019;70:838–843. doi: 10.1177/0003319719842682
 19. Ghadri JR, Kato K, Cammann VL, Gili S, Jurisic S, Di Vece D, Candrea A, Ding KJ, Micek J, Szawan KA, et al. Long-term prognosis of patients with takotsubo syndrome. *J Am Coll Cardiol*. 2018;72:874–882. doi: 10.1016/j.jacc.2018.06.016
 20. Nef HM, Mollmann H, Troidl C, Kostin S, Voss S, Hilpert P, Behrens CB, Rolf A, Rixe J, Weber M, et al. Abnormalities in intracellular ca²⁺ regulation contribute to the pathomechanism of takotsubo cardiomyopathy. *Eur Heart J*. 2009;30:2155–2164. doi: 10.1093/eurheartj/ehp240
 21. Scally C, Rudd A, Mezincescu A, Wilson H, Srivanasan J, Horgan G, Broadhurst P, Newby DE, Henning A, Dawson DK. Persistent long-term structural, functional, and metabolic changes after stress-induced (takotsubo) cardiomyopathy. *Circulation*. 2018;137:1039–1048. doi: 10.1161/CIRCULATIONAHA.117.031841
 22. Di Vece D, Citro R, Cammann VL, Kato K, Gili S, Szawan KA, Micek J, Jurisic S, Ding KJ, Bacchi B, et al. Outcomes associated with cardiogenic shock in takotsubo syndrome. *Circulation*. 2019;139:413–415. doi: 10.1161/CIRCULATIONAHA.118.036164
 23. Redfors B, Jha S, Thorleifsson S, Jernberg T, Angeras O, Frobert O, Petursson P, Tornvall P, Sarno G, Ekenback C, et al. Short- and long-term clinical outcomes for patients with takotsubo syndrome and patients with myocardial infarction: a report from the Swedish coronary angiography and angioplasty registry. *J Am Heart Assoc*. 2021;10:e017290. doi: 10.1161/JAHA.119.017290
 24. Templin C, Ghadri JR, Diekmann J, Napp LC, Bataiosu DR, Jaguszewski M, Cammann VL, Sarcon A, Geyer V, Neumann CA, et al. Clinical features and outcomes of takotsubo (stress) cardiomyopathy. *N Engl J Med*. 2015;373:929–938. doi: 10.1056/NEJMoa1406761
 25. Uribarri A, Nunez-Gil IJ, Conty DA, Vedia O, Almendro-Delia M, Duran Cambra A, Martin-Garcia AC, Barrionuevo-Sanchez M, Martinez-Selles M, Raposeiras-Roubin S, et al. Short- and long-term prognosis of patients with takotsubo syndrome based on different triggers: importance of the physical nature. *J Am Heart Assoc*. 2019;8:e013701. doi: 10.1161/JAHA.119.013701
 26. Jynge P, Brurok H, Asplund A, Towart R, Refsum H, Karlsson JO. Cardiovascular safety of mndpdp and mncl2. *Acta Radiol*. 1997;38:740–749. doi: 10.1080/02841859709172407
 27. Marti-Bonmati L, Fog AF, de Beeck BO, Kane P, Fagertun H. Safety and efficacy of mangafodipir trisodium in patients with liver lesions and cirrhosis. *Eur Radiol*. 2003;13:1685–1692. doi: 10.1007/s00330-002-1784-5
 28. Kume T, Akasaka T, Kawamoto T, Yoshitani H, Watanabe N, Neishi Y, Wada N, Yoshida K. Assessment of coronary microcirculation in patients with takotsubo-like left ventricular dysfunction. *Circ J*. 2005;69:934–939. doi: 10.1253/circj.69.934
 29. Bybee KA, Murphy J, Prasad A, Wright RS, Lerman A, Rihal CS, Chareonthaitawee P. Acute impairment of regional myocardial glucose uptake in the apical ballooning (takotsubo) syndrome. *J Nucl Cardiol*. 2006;13:244–250. doi: 10.1007/BF02971249